Available online at www.sciencedirect.com
SCIENCE DIRECT®
Journal of Power Sources 119–121 (2003) 979–985
JOURNAL OF POWER SOURCES
www.elsevier.com/locate/jpowsour

Mass transport limitation in implantable defibrillator batteries

C. Schmidt*, G. Tam, E. Scott, J. Norton, K. Chen
Medtronic Inc., Minneapolis, MN, USA

Abstract

Using cells with lithium reference electrodes, the power-limiting behavior in the lithium–SVO cell was shown to be due to a rapid voltage transition at the anode. A novel test cell was developed to explore the influence of current density, bulk $LiAsF_6$ concentration, separator type and separator proximity to the anode on the time to onset (τ) of the anode polarization. The results were found to follow a relationship, $i\tau^{1/2} \propto C_{bulk}$, consistent with the Sand equation. This relationship also predicts that the critical concentration of $LiAsF_6$, at which onset of the anode polarization occurs, is near the solubility limit of $LiAsF_6$ in our system (around 3.5–4.0 M). This general phenomenon was found to be quantitatively similar for two dissimilar separator types, and the anode polarization could also be induced in the absence of separator at high concentration and current density. However, it appears that τ decreases with closer proximity of the separator to the anode surface (i.e. cell stack pressure), suggesting that the effect of separator is to inhibit convective transport to and from the Li surface.
© 2003 Published by Elsevier Science B.V.

Keywords: Lithium; Battery; Silver vanadium oxide; Mass transport

1. Introduction

Lithium–silver vanadium oxide (Li–$Ag_2V_4O_{11}$ (Li–SVO)) primary batteries are used as power sources for implantable cardioverter-defibrillators (ICDs). These devices are used to monitor electrical activity in the heart, detect an arrhythmia, and deliver an appropriate therapy. The therapy can include a shock as high as 30–35 J. This is accomplished by first charging one or more capacitors to a high voltage and then discharging the capacitors through an electrical lead to the heart. As these arrhythmias can be life threatening, it is important that the therapy be delivered as quickly as possible after detection of the arrhythmia. Therefore, it is critical to minimize capacitor charge times by optimization of the capacitor charging circuit and the battery design. In addition, limiting the size of the implantable device minimizes the impact to the patient. Thus, understanding the factors that control battery rate capability is important so that the batteries can be operated near maximum power levels and designed with minimum volume.

In a previous study, we mapped the power capability of Li–SVO batteries by measuring voltage drop as a function of pulse current density and pulse duration [1,2]. At low current densities and short pulse durations, we observed a nearly linear *I–V* relationship. However, at high current densities and long pulse durations, we observed a rapid drop in voltage and a corresponding loss in power. This behavior was presumed to be due to mass transport limitations, but the source of the behavior was not investigated at that time. The proximity of the power loss region to the peak power region makes this behavior an important area of study that is the subject of this paper.

2. Experimental

A lithium anode was used in all electrochemical cells. The cathode was either silver vanadium oxide prepared as described earlier [2] or a lithium electrode. The electrolyte was $LiAsF_6$ in 50/50 (v/v) percentage of PC/DME with concentrations ranging from 0.5 to 3.0 M. All measurements were made at 37 ± 2 °C.

The electrolyte was characterized by measuring conductivity and viscosity as a function of $LiAsF_6$ concentration. The $[Li^+]$ values were confirmed by using inductively coupled plasma–mass spectrometry (ICP–MS). Conductivity (σ) measurements were carried out by a Hewlett Packard 4263A LCR meter and a YSI 3403 conductivity cell (cell constant: 1.0 cm^{-1}). Dynamic viscosity (η) was measured using a Brookfield DV-IT viscometer with a type UL#00 spindle. During conductivity and viscosity measurements, the temperature of the electrolyte samples was controlled by immersing the containment vessels in a circulating water bath.

* Corresponding author.
E-mail address: craig.schmidt@medtronic.com (C. Schmidt).

0378-7753/03/$ – see front matter © 2003 Published by Elsevier Science B.V.
doi:10.1016/S0378-7753(03)00306-9

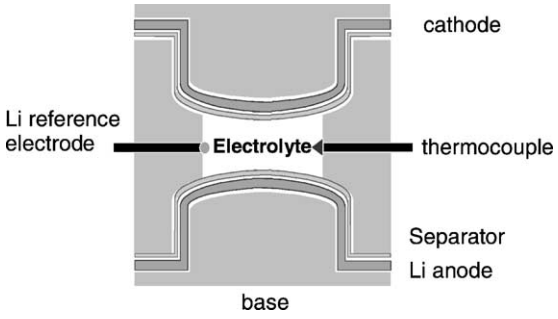

Fig. 1. Arc cell design.

Three basic electrochemical cell types were used. The first cell type was a typical ICD battery constructed as described previously [3]. In some cases, a small lithium reference electrode was located between the anode and cathode. The reference electrode was accessed via a separate hermetic feed through in the battery case. Both electrodes were sealed in a polypropylene micro-porous separator. The electrolyte was 1 M $LiAsF_6$ in 50/50 (v/v) percentage of PC/DME. The second cell type was constructed in a sealed glass vessel (''jar cell'') having 2 cm^2 lithium and SVO electrodes separated by about 1 cm and a lithium reference. In some jar cells, the anode was encased in a separator ''bag'', and in others it was not. The third cell type (''arc cell'') is shown in Fig. 1. This cell was constructed of Delrin^{TM} and was designed specifically for this study. Each electrode holder could accommodate either a lithium or SVO electrode. In the case of SVO, the electrode material was pressed onto a titanium grid current collector [3]. The base of the electrode holder was designed with a slight convex arc (7.62 cm radius) rather than with a perfectly planar geometry. When the top of the electrode holder is in place, the arc forces the separator to be held tautly against the electrode, simulating the proximity of the separator to the electrode in a typical ICD battery. This close proximity could neither readily be achieved with a planar electrode nor with the jar cell described earlier. The cell had access holes for a lithium reference electrode and a thermocouple. The access holes were equidistant between the anode and cathode, and the reference and thermocouple were extended about 2 mm into the cell interior. The exposed area of both the anode and cathode electrodes was 2 cm^2, and the inter-electrode spacing was 0.5 cm at the closest point.

Two separator types were studied. These are described hereafter as ''MP'' and ''MP/NW.'' The MP material is micro-porous polypropylene film with a thickness of approximately 25 μm and a porosity of approximately 0.45. The MP/NW material has a micro-porous layer essentially identical to the MP, but also has a non-woven layer dot-bonded to the micro-porous layer. The total thickness is approximately 90 μm, and its porosity is reported as 0.45 by the vendor. However, we believe the porosity of the non-woven layer is approximately 0.8, while the porosity of the micro-porous layer is around 0.45. Great care was necessary in preparation of cells, to ensure reproducible measurements free from artifacts due to incomplete wetting of the separators. At electrolyte concentrations above 1 M, separators were found to be prone to non-uniform or incomplete wetting, as evidenced by anomalously high cell resistance. To prevent this effect, separators were pre-wet by first soaking in 1 M electrolyte solution and then in the solution concentration of interest prior to cell assembly. After assembly, cells were pre-filled with a syringe, followed by vacuum filling by placing them in a bell jar while immersed in electrolyte.

Current–voltage polarization experiments were carried out using either of the following instruments (hereafter referred to as potentiostats for simplicity): a Solartron 1480 multistat with auxiliary voltage–temperature module; or an EG&G/PAR 273 potentiostat. The choice of instrument depended on a balance between the need for the higher compliance of the PAR or the auxiliary voltage–temperature measurement capability of the Solartron. The configuration of attachment of electrical leads to the various cell electrodes varied, depending on the cell and potentiostat types. For Li|Li arc cells, the whole cell voltage is presented, rather than anode versus reference. This was found to give the most consistent representation of the anode voltage, because the uncontrolled shift in the reference voltage was found to be greater than the shift in cathode voltage. The reference potential was found to be unstable under dynamic conditions due to a combination of *I–R* and concentration effects. This is believed to be exacerbated by the relatively short inter-electrode spacing (causing the reference electrode to be subject to concentration and potential gradients in the vicinity of the active electrodes) as well as run-to-run variability in reference electrode placement (estimated at ±1 mm) within the cell.

3. Results and discussion

3.1. Preliminary study

Fig. 2 shows the potential of the anode and cathode of an ICD battery versus its lithium reference electrode during a high current density pulse. The most striking feature of this plot is the sharp rise of the anode potential after about 50 s. This transition occurs at shorter times as current density is increased. The rapid polarization is qualitatively similar to that seen in our previous study [1,2]. The cathode potential during the same period shows only a gradual decline with only a slight indication of a mass transport limit near the end of the pulse. However, subsequent testing showed that the decline in cathode voltage is likely an artifact associated with the reference electrode in this cell configuration.

The anode polarization was investigated in jar cells, where a greater physical separation could be achieved between the anode and cathode. When the anode was not encased in separator (Fig. 3a), its potential was stable at high current densities and long pulse durations. However, when

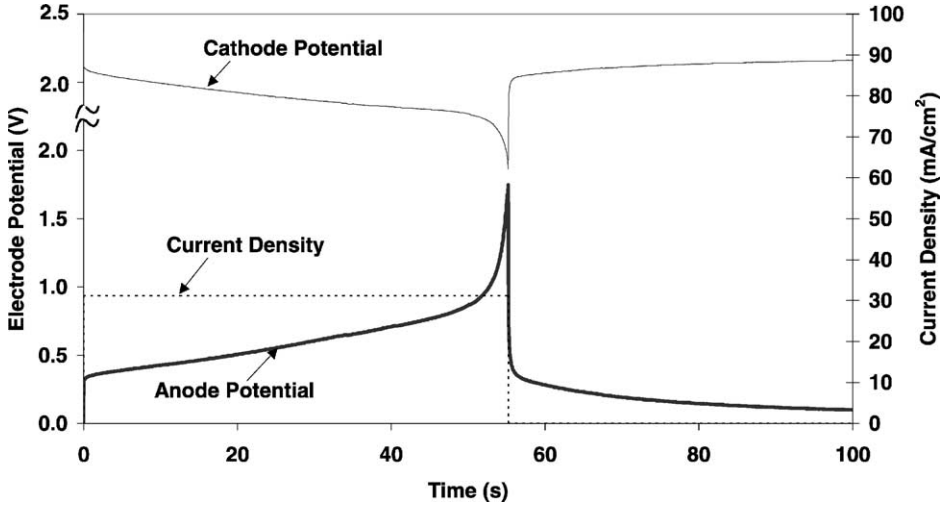

Fig. 2. Li and SVO potential vs. a Li reference in an ICD battery during a high current density pulse.

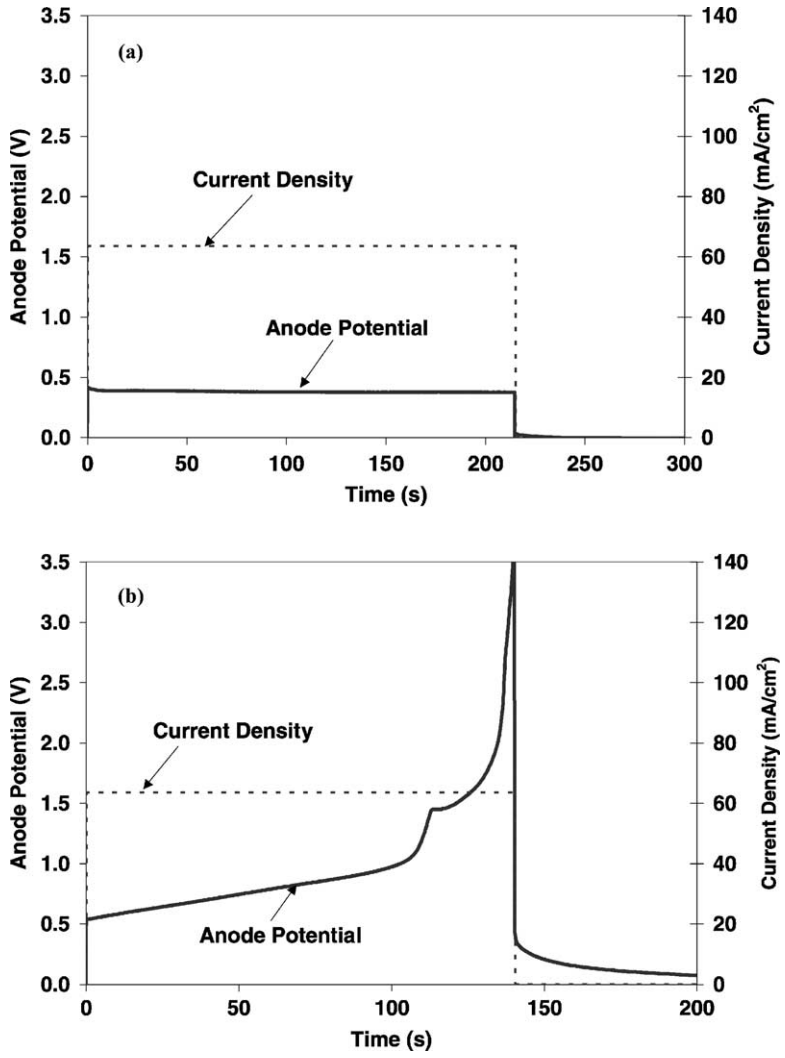

Fig. 3. Li anode potential vs. a Li reference in a jar cell during a high current density pulse: (a) no separator on anode; (b) anode encased in separator. Electrolyte concentration was 1.0 M and temperature was 37 °C.

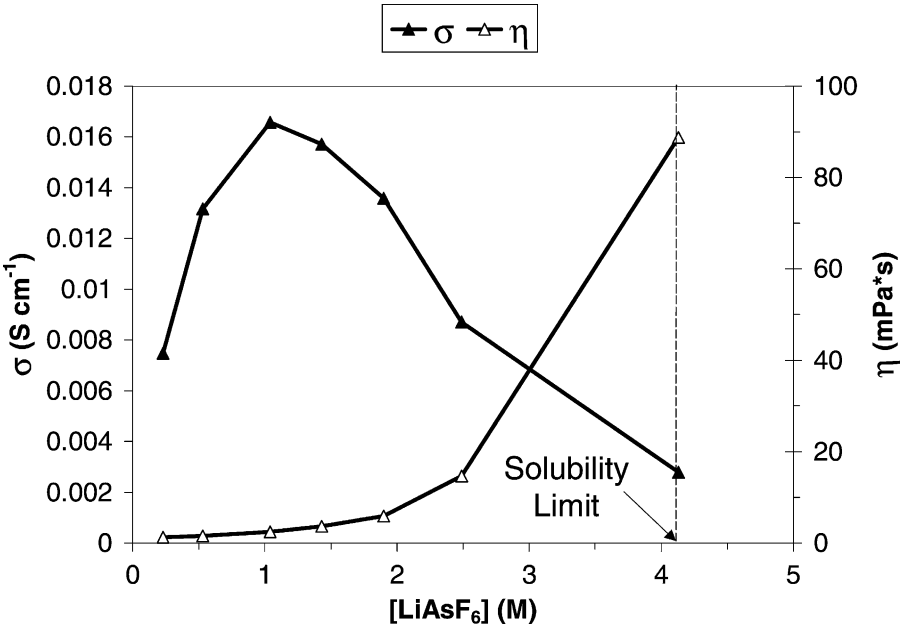

Fig. 4. Specific conductivity and viscosity of $LiAsF_6$–PC–DME electrolyte as a function of concentration.

the anode was encased in the MP–NW separator (Fig. 3b), the polarization behavior was qualitatively similar to that observed in the defibrillator battery, although the current density and pulse duration required to observe the transition behavior were significantly higher than in the ICD battery. One difference between the jar cell and the ICD battery was that the separator could not be held in close contact with the lithium anode in the jar cell as it is the ICD battery.

These observations suggested that the rapid change in anode polarization might be associated with the development of highly concentrated and low conductivity electrolyte at the anode. During an extended high current density pulse, the $LiAsF_6$ concentration at the anode increases due to the non-unity value of the lithium transference number. The micro-porous separator inhibits convective mass transport away from the anode. At a critical $LiAsF_6$ concentration, the conductivity of the electrolyte drops precipitously, resulting in the polarization behavior observed in Figs. 2 and 3b. The rapid drop in anode potential when the current pulse is terminated also suggests an Ohmic nature of the voltage transition. When a separator barrier is not present (Fig. 3a), there is sufficient convective mass transport to prevent the critical concentration from being attained at reasonable current densities. The longer transition time and higher current density required in the jar cell versus the ICD battery may be the result of a larger gap between the separator and the lithium electrode in the jar cell than in the tightly wound ICD battery.

3.2. Conductivity and viscosity of the electrolyte

To more fully test this hypothesis, it was necessary gather more information about the conductivity of the electrolyte. The $LiAsF_6$–PC–DME electrolyte conductivity and viscosity are shown as a function of $LiAsF_6$ concentration in Fig. 4. Note that the 1 M concentration used in our ICD batteries provides the optimum conductivity. The same data are shown in Fig. 5 by plotting the product of specific conductivity and viscosity versus electrolyte concentration. The linear relationship at low electrolyte concentrations suggests that equivalent conductance of the electrolyte is primarily an inverse function of the viscosity (Nernst– and Stokes–Einstein relations) and is relatively independent of other concentration effects [4]. The deviation from linearity at higher concentrations is in the opposite direction to our expectations, indicating a higher conductivity than would be anticipated at these high viscosities. While the conductivity does decrease significantly as concentration is increased, the

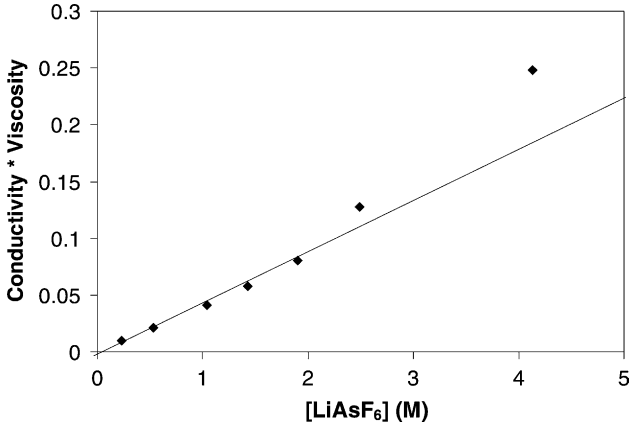

Fig. 5. Product of conductivity and viscosity of $LiAsF_6$–PC–DME electrolyte as a function of concentration. Straight line represents idealized behavior.

decrease does not seem to be entirely sufficient to explain the large change in anode potential during a high current pulse. However, it becomes exceedingly difficult to work with solutions above 3.5 M because they are near the solubility limit and have a gel-like consistency. It is possible that the apparent high resistance at the anode occurs when the solubility limit is exceeded.

3.3. Effect of current density and electrolyte concentration

In order to more closely approximate the physical relationship between the anode and separator found in the ICD battery configuration, the test cell shown in Fig. 1 was designed and constructed. The cell was assembled using MP–NW separator on the anode with electrolyte concentrations of 0.5, 1.0, 1.25, 2.0, 2.5, and 3.0 M. In this study, a lithium electrode was used for both the anode and cathode in order to simplify construction. After the cell had equilibrated at 37 °C, it was subjected to current pulses of 60, 70, and 80 mA/cm^2. A 15-min quiescent period was allowed between pulses. A subset of the results of these studies is shown in Fig. 6. The data clearly illustrate that the onset time of anode polarization decreases with increasing current density and increasing electrolyte concentration. It should be noted that the initial voltage ($t = 1$ s) is a result of the iR drop due to the 0.5 cm gap between electrodes, and that the voltage plateau around 11 V is a limitation of the potentiostat. The same characteristics are present in Figs. 8 and 9.

We defined the transition time, τ, by the intersection of a line tangent to the pre-polarization voltage region and another line tangent to the post-polarization voltage region. We explored the possibility that the transition time showed an inverse relationship to either current ($i\tau = \text{constant}$) or the square of the current ($i^2\tau$ or $i\tau^{1/2} = \text{constant}$). The former relationship would indicate that the onset of polarization is related to the total quantity of charge passed while the latter would indicate diffusion control. For a given electrolyte concentration, we found that the product, $i\tau^{1/2}$, was relatively independent of current density. When $i\tau^{1/2}$ is plotted versus the bulk concentration of electrolyte, a linear relationship is observed over most of the concentration range (Fig. 7). This relationship can be described by Eq. (1) which has the same functional form as the Sand equation [5].

$$i\tau^{1/2} = mFA(C_{\text{crit}} - C_{\text{bulk}}) \quad (1)$$

where m is a mass transfer coefficient, F the Faraday's constant, A the the electrode area, C_{bulk} the bulk concentration of electrolyte and C_{crit} the critical concentration at the electrode surface at which the anode polarization occurs. With this interpretation, the x-axis intercept represents the critical surface concentration. Interestingly, this concentration not far from the solubility limit of $LiAsF_6$ (approximately 4 M), which may suggest that precipitation at the lithium surface is involved in the polarization of the anode. It is somewhat surprising to discover this conformance to the Sand equation-type behavior given that there is no support-

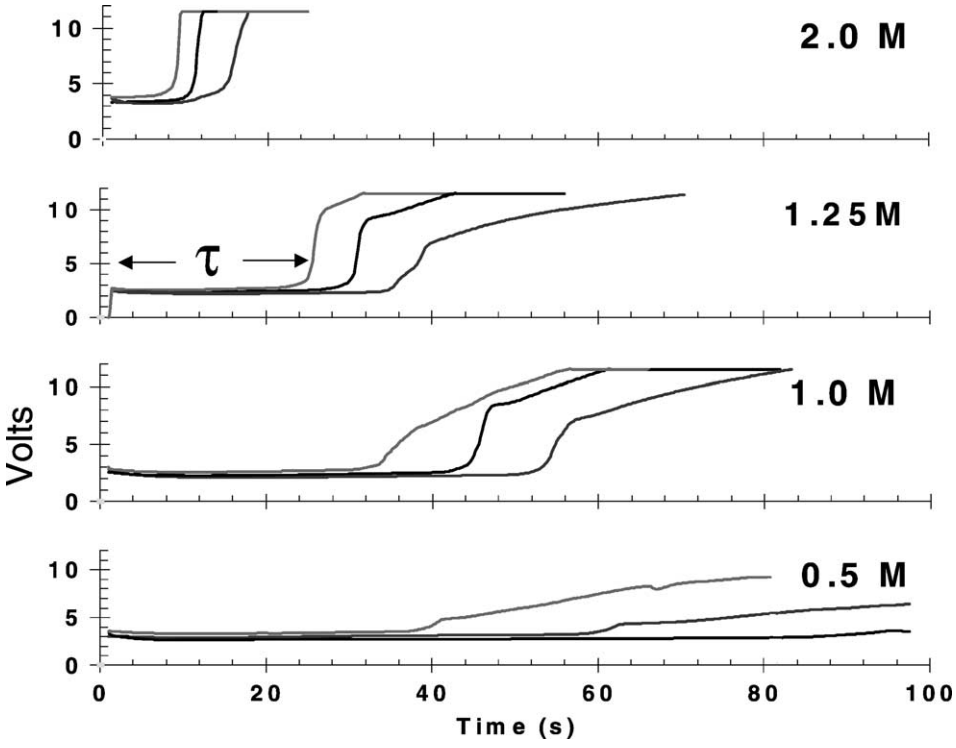

Fig. 6. Transition behavior as a function of current density and electrolyte concentration in the arc cell using MP–NW separator. The top line at each graph represents 80 mA/cm^2, the middle line 70 mA/cm^2, and the bottom line 60 mA/cm^2. Current was applied at $t = 1$ s.

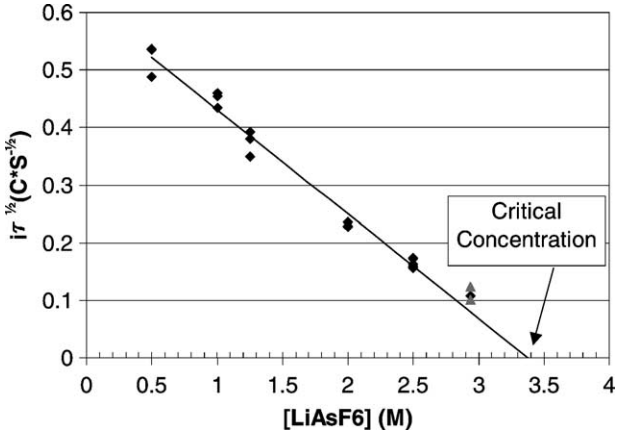

Fig. 7. The $i\tau^{1/2}$ vs. electrolyte concentration. The data at each concentration represent three current densities.

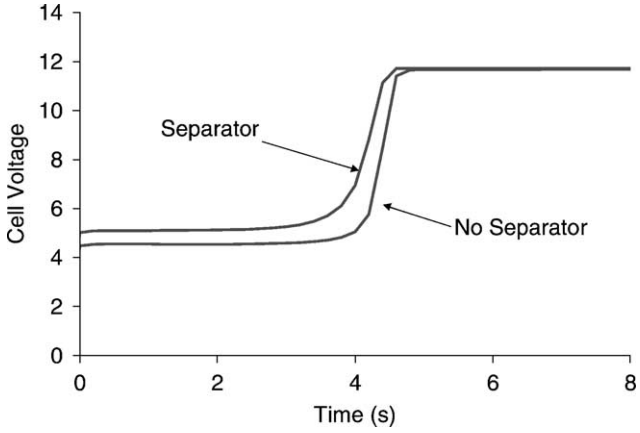

Fig. 9. Demonstration of similar results with and without separator at high concentration and high current density. Concentration of electrolyte was 2.5 M and current density was 80 mA/cm^2.

ing electrolyte and that the solution viscosity, and hence diffusion coefficients, change dramatically over this range of concentrations. The deviation from linearity observed at 3 M may be a result of these effects. Nonetheless, the data in Fig. 9 and the functional form provided by Eq. (1) give valuable insight about the nature of the anode polarization.

3.4. Effect of separator proximity to lithium

Fig. 8 compares voltage versus time behavior under three conditions: no separator on the lithium anode, a taut separator held in place by the test fixture, and a separator pressed onto the lithium to maintain a more intimate contact. (The non-woven layer of the MP–NW separator used in this experiment sticks to the surface of the lithium if it is pressed in place.) Even when no separator is placed over the lithium, a small transition in voltage can still be observed at about 60 s. However, the magnitude of the voltage transition is very small compared to that observed with separator. The proximity of the separator to the lithium is clearly a significant factor, with a more intimate separator contact yielding a shorter time to onset of polarization. These results suggest that stack pressure may strongly affect the conditions under which this limiting behavior is observed in a battery. A specific example is given later in this paper.

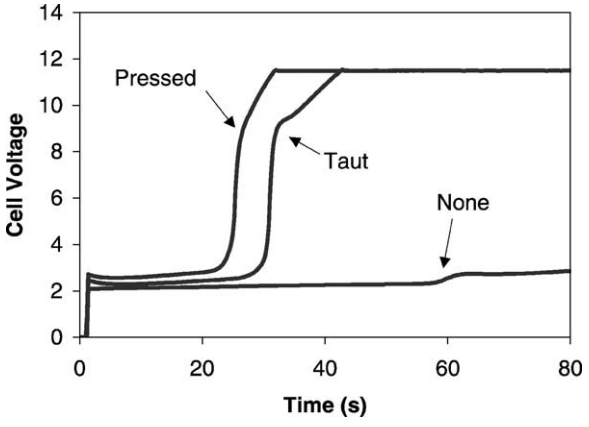

Fig. 8. Effect of proximity of separator to lithium. The MP–NW separator was either pressed onto the lithium, held taut against the lithium, or not present. Electrolyte concentration was 1.25 M and current density was 70 mA/cm^2. Current pulse was applied at $t = 1$ s.

The effect of separator proximity becomes much less important as electrolyte concentration and/or current density is increased. This is illustrated in Fig. 9. At a concentration of 2.5 M and a current density of 80 mA/cm^2, there is little difference between the polarization behavior with or without a separator. At high concentrations and high current densities, the transition time is short enough that convection is not a significant factor. Thus, similar behavior is observed with and without a separator.

3.5. Effect of separator type

In spite of the very different structures and dimensions of the MP and MP–NW separators, we observed no significant difference in the observed time to onset of polarization with the two separators. Once again, this is strong supporting evidence that the effect of separator is merely to inhibit convective mass transport.

Additional insight is gained by a comparison of the performance of Li–SVO ICD batteries constructed with these two separators (Fig. 10). It should be noted that while the two batteries are not completely identical in design, the experiments were carried out at identical anode current densities. In this case, the battery constructed with the MP separator exhibited considerably longer transition times than the battery constructed with the MP–NW separator. At first glance, these data seem to be contradictory with the data gathered in the test cell. However, there are several important differences that should be noted. Both the types of cells are constructed by heat-sealing a separator "bag" around both the anode and the cathode. In the case of the MP–NW material, the separator is pressed onto the lithium to facil-

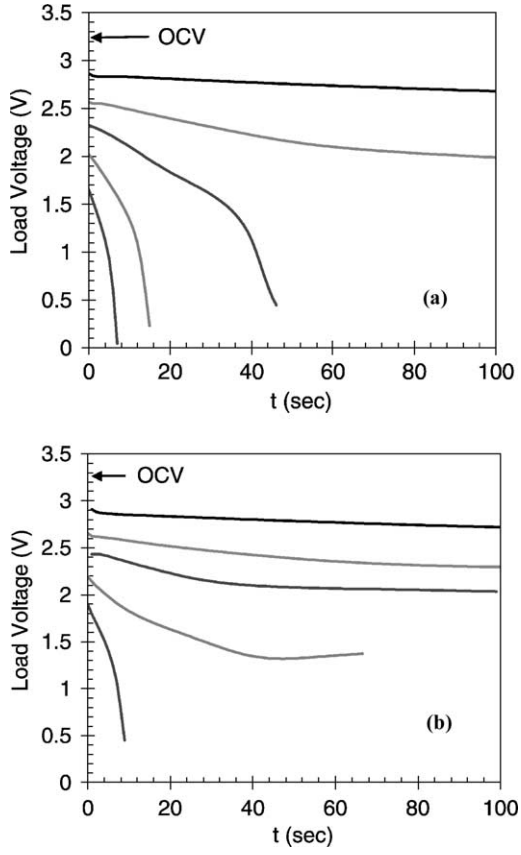

Fig. 10. Comparison of behavior of: (a) MP–NW, and (b) MP separators, in Li–SVO ICD batteries as a function of current density. Current densities are (starting with the uppermost curve) 10, 25, 40, 60, and 80 mA/cm^2.

itate handling. This pressing procedure is not used with the MP separator for the reasons noted earlier. In addition, when the ''bagged'' electrodes are wound, the separator does not necessarily maintain a tight contact to the lithium in all areas. This is particularly true for the MP material. Finally, while the SVO cathode swells during discharge, its thickness increase matches the declining thickness of the lithium electrode. There is no net swelling of the cell stack during discharge. The separator–lithium contact that exists at the beginning of discharge is likely to be maintained throughout discharge. Therefore, the results obtained with these batteries are similar to the behavior observed in Fig. 8, where the proximity of the separator to the lithium was shown to be a significant factor.

4. Conclusions

The power-limiting behavior observed in Li–SVO batteries occurs at the lithium anode for electrolyte concentrations of 1 M or greater. It is an indirect result of concentration polarization at the anode during a high current density pulse. As the electrolyte concentration approaches saturation at the electrode surface, the conductivity drops abruptly causing a large voltage transition. As electrolyte concentration or current density is increased, this polarization is observed at shorter times.

The primary effect of separator on the anode polarization behavior is to inhibit convective mass transport near the electrode surface. This is illustrated by several observations. At lower electrolyte concentrations and low current density, the proximity of the separator to the lithium is an important factor, while at higher electrolyte concentrations and high current density similar transition times are observed both with and without separator. In addition, separator thickness has little effect on the behavior. Finally, in the presence of separator the effect of electrolyte concentration and current density is consistent with a diffusion controlled process (i.e. concentration polarization at the lithium electrode). The product of current with the square root of transition time, $i\tau^{1/2}$, is independent of current at a given electrolyte concentration and declines linearly with increasing concentration. In spite of the absence of a supporting electrolyte and diffusion coefficients that certainly vary widely over the range of electrolyte concentrations studied, the relationship between current density, transition time, and concentration is accurately described (at concentrations as high as 2.5 M) by an equation having the same functional form as the Sand equation.

References

[1] J. Norton, C. Schmidt, in: Proceeding of the Symposium on Batteries for Portable Applications and Electric Vehicles, C.F. Holmes, A.R. Landgrebe (Eds.), PV 97–18, The Electrochemical Society, 1997, pp. 389–393.
[2] A. Crespi, C. Schmidt, J. Norton, K. Chen, P. Skarstad, J. Electrochem. Soc. 148 (2001) A30–A37.
[3] A. Crespi, S. Somdahl, C. Schmidt, P. Skarstad, J. Power Sources 96 (2001) 33–38.
[4] J.O'M Bockris, A.K.N. Reddy, Modern Electrochemistry I—Ionics, 2nd ed., Plenum, New York, 1998, pp. 454–457.
[5] A.J. Bard, L.R. Faulkner, Electrochemical Methods, Wiley, New York, 1980, pp. 252–255.